

Injectable Biopolymer-hydroxyapatite Hydrogels: Obtaining and their Characterization

L.B. Sukhodub^{1*}, G.O. Yanovska², V.M. Kuznetsov², O.O. Martynyuk², L.F. Sukhodub²

¹ *SI "Institute of Microbiology and Immunology, the Mechnikov I.I. AMS of Ukraine". 14/16, Pushkinska St., 61057 Kharkiv, Ukraine*

² *Sumy State University, 2, Ryskogo-Korsakova St., 40007 Sumy, Ukraine*

(Received 21 December 2015; published online 15.03.2016)

Hydrogels based on hydroxyapatite (HA) and Chitosan (CS) with addition of sodium alginate (Alg) were synthesized by *in situ* precipitation method. Structure, morphology, chemical and phase composition of the HA/CS and HA/CS/Alg hydrogels were characterized by TEM, FTIR and XRD. Hydrogels consist of low crystallinity calcium deficient hydroxyapatite (JCPDS 9 432), the needle-like crystallites have an average size 25 nm. The introduction of Alginate powder into HA/CS hydrogel solution demonstrate the viscosity enhancing of the HA/CS hydrogel due to polyelectrolyte reaction between Alginate and Chitosan macromolecules. Two natural polymers and partially released from hydroxyapatite Ca^{2+} ions formed a matrix by crosslinking the polymer macromolecules through hydroxyl, amino and carbonyl groups. These processes promote the formation of a more stable structure of HA/CS/Alg hydrogel as compared to HA/CS. The structural integrity and degradation tests have demonstrated that HA/CS/Alg_{1.0} saved its initial shape in 7 days of shaking in SBF solution, meanwhile for HA/CS, a structural decay was observed. The HA/CS hydrogel had completely lost its volume support after 1 day shaking in SBF. Thus, the ability of HA/CS hydrogel to maintain its shape with implantation into bone tissue defect may be enhanced with alginate addition, but alginate content more than 1 w/w % reduces the hydrogel plasticity, increases the swelling and accelerates the shape decay.

Keywords: Hydroxyapatite, Chitosan, Sodium alginate, Hydrogels.

DOI: 10.21272/jnep.8(1).01032

PACS numbers: 87.85.J – , 87.64.Bx, 87.64.Ee

1. INTRODUCTION

Hydrogels are soft and wet materials, composed of a three-dimensional polymer network in which a large amount of water molecules are interposed [1]. Some recent studies have indicated that hydrogels, especially those derived from natural proteins and polysaccharides, are ideal scaffolds for tissue engineering, since they not only offer several advantages over synthetic polymers and inorganic scaffolds but also provide a three-dimensional (3-D) environment and morphology close to the extracellular matrix of native tissues [1-3]. Because of their hydrophilicity and other unique properties, such as biocompatibility, biodegradability, and responsiveness to various kinds of stimuli, hydrogels could be used as scaffolds for tissue engineering [4-5], carriers for drug delivery [6]. However, most hydrogels suffer from a lack of mechanical strength. To obtain hydrogels with a high degree of toughness, a number of techniques have recently been proposed, including the double network (DN) hydrogels [1, 7-9] and the nanocomposite hydrogels [10].

A molecular control on the morphology, size, and anisotropy of the inorganic crystals and their uniform distribution over the organic phase are some of the main goals in the biomimicking process. Polymers containing polar functional groups such as $-\text{COOH}$, $-\text{CH}$, $-\text{CH}_2$, $-\text{PO}_4\text{H}_2$, and $-\text{OH}$ have been found to be useful in this regard since these ionizable side groups provide a greater affinity to positive calcium ions and the result nucleation of HA. Some of more recent attempts in the *in situ* mineralization technique have used of polymeric additives due to their calcium binding properties [11].

Chitosan can form polymeric matrix with alginate through protonated amino groups NH_2^{3+} and COO^- , Fig. 1 [12].

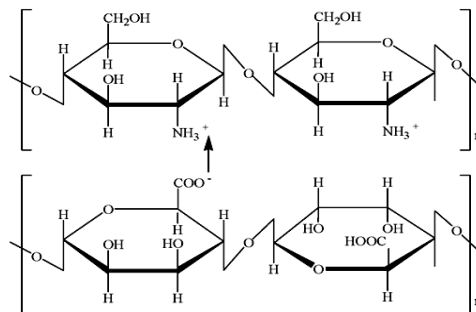


Fig. 1 - Structures and scheme of Chitosan-Alginate Interaction

Nanocomposite hydrogels based on polysaccharides CS, Alg are very promising materials for tissue engineering. Sodium alginate form hydrogels via ionotropic crosslinking in the presence of divalent cations such as calcium [13]. Hydrogels based on calcium-crosslinked alginate have been widely investigated for various drug delivery purposes and injectable systems [13-16]. Since CS has been reported to be biodegradable [17] and HA is able to release calcium ions in a physiological environment, it is reasonable to assume that the addition of alginate to HA/CS could lead to *in situ* formation an injectable HA/CS/Alg composite hydrogel, which could combine the advantages of Alg, CS and HA, especially maintaining the bioactivity of CS, osteoconductivity of HA and the elasticity and porous structure of the Alg hydrogel.

* l.sukhodub@gmail.com

Hydrogels based on HA and CS with addition of sodium alginate are proposed in this study. Two natural polymers form a matrix by crosslinking their macromolecules through amino and carbonyl groups. Ca^{2+} ions, partially released from hydroxyapatite, are involved in the process of crosslinking of the alginate matrix. These processes contribute to the formation of a more stable hydrogel structure. Therefore, in this study, HA/CS/Alg composite hydrogels were prepared by self-crosslinking of alginate with Ca^{2+} ions released from HA/CS hydrogel and simulated body fluid (SBF) solution without employing any extraneous crosslinking agents.

2. MATERIALS & METHODS

2.1 Materials

The next chemicals were used: Sodium alginate (low viscosity, E407, China), calcium chloride CaCl_2 , ortho phosphoric acid H_3PO_4 (Sinopharm Chemical Reagent Co., Ltd.), Chitosan (molecular weight 150 kDa, D.D. 85 %, Fluka, Germany). All reagents were analytically grade.

2.2 Preparation of the Injectable Hydrogel

HA/CS hydrogel was synthesized by a wet chemistry. Two solutions were prepared for synthesis: the first one: 100 mL CaCl_2 with concentration 0.1 M, pH was adjusted up to 11.0 by addition of 10 M NaOH solution; the second one: chitosan was dissolved in 100 ml 0.06 M H_3PO_4 in quantity, which provides its content in the final material by 40 % in relation to the HA. The second solution was added drop by drop to the first one with mixing and heating at 60 °C during 10 minutes. The pH value was adjusted up to 7.4. After aging for 24 hours a resulted suspension was washed with distilled water and centrifuged to obtain the product in form of HA/CS hydrogel with moisture degree about 90 %. It can be used as injectable hydrogel in the as-prepared form.

Two polymer containing hydrogel HA/CS/Alg was prepared by adding different amounts (1 and 1.5 w/w %) of sodium alginate powder into wet (90 % moisture) HA/CS hydrogel. Sodium alginate powder was dispersed homogeneously in a HA/CS by mixing ultrasonically and left for reaction during 24 hours. Antibacterial action was reached by sterilization of the material under ultraviolet light $\lambda = 280$ nm for 15 min.

2.3 Swelling and Degradation Study

For swelling and degradation study HA/CS and HA/CS/Alg composites with various alginate content were partially dried at 37 °C to get humidity about 74 w/w % and examined in cubic form. All pre-weighed samples were enclosed in metallic sieves in glass vessels with 200 mL SBF buffer solution at a ratio of 0.022 g mL^{-1} . The glass vessels with metallic sieves and samples were taken into shaker at 37 °C for 5 days with shaking 50 rpm.

The samples were removed after 24, 48, 72, 96 and 120 hours, carefully filtered and weighed. The degradation percentage (D_w) was calculated using the following equation:

$$D_w\% = (W_0 - W_t)/W_0 \times 100 \quad (2)$$

The precise analysis of the swelling behavior was additionally performed by measuring the changes in sample weight during first 5 minutes of immersion time in SBF with interval 1 minute. The swollen samples were weighed after blotting with a filter paper to remove the surface water. The swelling ratio (S_w) of the hydrogel was calculated using the following equation [18]:

$$S_w\% = (W_t - W_0)/W_0 \times 100 \quad (1)$$

where W_0 is the initial weight, W_t is the final weight of the swollen hydrogel.

The data points represent the mean \pm SD from three independent swelling experiments.

2.4 TEM Analysis

The structural morphologies of the synthesized polymer-hydroxyapatite composites was observed by transmission electron microscope (TEM-125K, SELMI, Sumy, Ukraine). The accelerating voltage was equal to 90 kV. Support copper ($30 \times 30 \mu\text{m}$) and nickel ($50 \times 50 \mu\text{m}$) nets were used for the arrangement of objects in the object plane of the TEM objective lens. Since the objects sizes were less than the net holes, they were placed on thin, transparent for electrons, continuous carbon films of the thickness of 20 nm. The experimental samples were deposited on the support net with the carbon film prefastened in a grid due to dispergation of suspension by ultrasonic method. The suspension was obtained by the gel solution method by distillate water.

2.5 XRD Analysis

The structural crystallinity of all precipitates were examined using an X-ray diffractometer DRON-3 (Burevestnik, www.bourestnik.ru) connected to a computer-aided system for the experiment control and data processing. The Ni-filtered $\text{CuK}\alpha$ radiation (wavelength 0.154 nm) with a conventional Bragg-Brentano θ - 2θ geometry was used. The current and the voltage of the X-ray tube were 20 mA and 40 kV respectively. The samples were scanned in the continuous mode at a rate of $2.0^\circ/\text{min}$ in 2θ range of 10° to 60° . All experimental data was processed by means of the program package DifWin-1 (Etalon-TC, www.specord.ru). Identification of crystal phases was done using a JCPDS card catalog (Joint Committee on Powder Diffraction Standards, www.icdd.com).

2.6 FTIR Analysis

The Fourier-transform infrared (FTIR) spectra were collected for the tablets of samples with KBr using spectrophotometer SPECTRUM ONE (PerkinElmer). For analysis hydrogels samples dried at 37 °C have been used.

3. RESULTS & DISCUSSION

3.1 Microscopy

The structural morphologies of the HA/CS were examined using TEM (Fig. 2). The HA crystallites in

composites are needle-like with average size about 30 nm. Upon preparation of HA/CS/Alg nanocomposite a sodium alginate was introduced into a reaction system after the formation of HA crystallites in HA/CS and did not affect their nanostructure. Therefore, structure characteristics obtaining by microscopy, as well as XRD were demonstrated only for HA/CS, and not for HA/CS/Alg system.

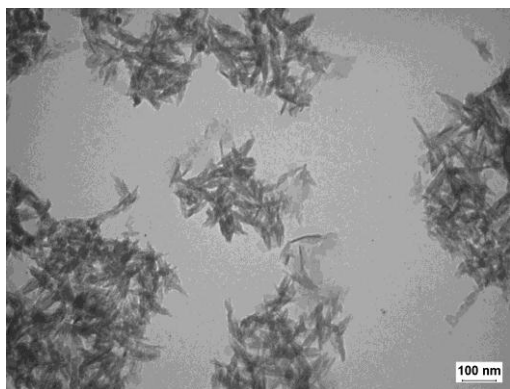


Fig. 2 – HA/CS composite: the TEM image of HA crystallites

3.2 XRD Analysis

X-ray diffraction spectra of the row (dried at 37 °C) and annealed (900 °C, 1 hour) samples are shown in Fig. 3. The phase composition of the row sample consists of low-crystallinity hydroxyapatite (JCPDS 9-432). The average crystallite sizes were calculated by the Scherrer equation [20] in (0 0 2) and (0 0 4) planes. Due to the presence of two peaks corresponding to the crystallographic planes lying parallel in the same direction, i.e. [0 0 c], it was possible to separate contributions from small sizes of coherent-scattering regions and the presence of microstrains into the peak broadening using the conventional approximation method [21].

The results (Table 1) show significant amounts of

Table 2 – Structural parameters of the annealed samples

| Sample | L (Scherrer), nm | | | | | | | C, % | |
|---------------|---------------------|---------|----------|---------|--------------------|---------|---------|------|------|
| | TCP (JCPDS 70-2065) | | | | HA (JCPDS 82-1943) | | | TCP | HAP |
| | (2 1 4) | (3 0 0) | (0 2 10) | (2 2 0) | (2 1 1) | (1 1 2) | (2 1 3) | | |
| HA/CS, 900 °C | 50 | 52,8 | 53,5 | 50,7 | 44,1 | 48,2 | 51,3 | 67,8 | 32,2 |

3.3 FTIR analysis

FTIR analysis was performed to evaluate the functional groups of Chitosan and synthesized composites with HA and shown in Fig. 4. The main characteristic wave number of this nanocomposites are presented in Table 3.

FTIR spectrum of pure HA (is not given) shows a peaks around 3431 cm⁻¹ and 630 cm⁻¹ corresponding to stretching vibration of the hydroxyl group [24]. Characteristic peaks at around 600 cm⁻¹, 961 cm⁻¹, 1037 cm⁻¹ and 1096 cm⁻¹ are due to the bending and stretching modes of P–O vibrations in the phosphate network [25, 26]. The peak 876 cm⁻¹ in HA/CS composite spectrum is a carbonate band mode, that indicates substitution of PO₄³⁻ for CO₃²⁻ in hydroxyapatite [24].

The spectrum of unmodified chitosan showed characteristic peaks of Amide I at 1667 cm⁻¹ (C=O stretch-

Table 1 – Structural parameters of the initial sample

| Sample | L (Scherrer), nm | | Approximation Method | |
|------------|------------------|---------|----------------------|-----------------------|
| | (0 0 2) | (0 0 4) | L, nm | $\epsilon \cdot 10^3$ |
| HA/CS, raw | 25,7 | 22,9 | 12,1 | 3 |

microstrains due to the presence of chitosan in the composite leading to the decrease of crystallinity [22].

Two phases were identified for the annealed sample – tricalcium phosphate (TCP) (JCPDS 70-2065) and hydroxyapatite (JCPDS 9-432). The heat treatment was performed to analyzed Ca / P ratio in the row sample [22], therefore the obtained results indicate calcium deficiency in it. The average sizes of crystallite increased more than twice (Table 2) due to the recrystallization process. The quantitative phase analysis was performed by Chung method [23].

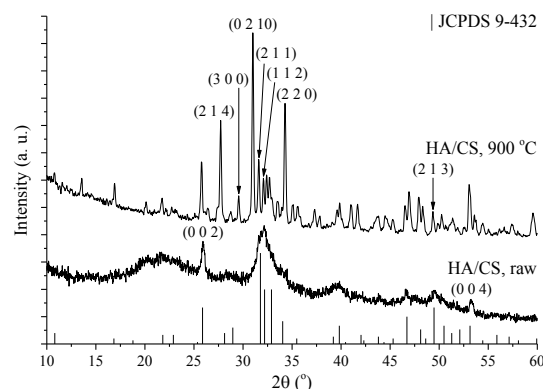


Fig. 3 – X-ray diffraction spectra of HA/CS composite

The quantitative elemental analysis was performed using the regression procedure for calcium and phosphorous to determine their atomic ratio, i.e. Ca / P. The obtained results, show that synthesized hydroxyapatite was as calcium deficient mineral with Ca / P = 1.41.

ing), Amide III at 1384 cm⁻¹ (C–N stretching coupled with NH in plane deformation) and CH₂ wagging coupled with OH in plane deformation at 1326 cm⁻¹.

The peak at 1599 cm⁻¹ belongs to the bending vibrations of the N–H and C–N (Amide II band) The peaks at 1422 belong to the N–H stretching of the amide and ether bonds [27]. The peaks at 1031 cm⁻¹ and 1082 cm⁻¹ indicate the C–O stretching vibration in the primary and secondary hydroxyl groups in chitosan respectively [28, 29].

For CS/HA composite it was observed the intensity decrease and shift of the peak at 1326 cm⁻¹ in chitosan to 1310 cm⁻¹ and disappearance this peak after 6 day of the nanocomposite immersion in SBF solution, that may indicate partial phosphorylation of hydroxyl groups with further formation of calcium phosphates in SBF solution with the participation of Ca²⁺ ions.

Table 3 – Characteristic wave number of HA, CS, HA/CS nanocomposite, HA/CS nanocomposite after finding 6 days in SBF solution

| Functional groups | Type of compounds and corresponding vibration peaks (wave numbers) | | | |
|--|--|------|-----------------------------|---|
| | HA | CS | HA/CS nanocomposite | HA/CS nanocomposite (after SBF solution) |
| –PO ₄ ³⁻ | 564 | | 561 | 561 |
| | 952 | | 960 | 963 |
| | 1033 | | 1029 | 1030 |
| | 1080 | | 1098 shoulder | 1098 shoulder |
| –OH- | 3431 | | 3429 | 3419 |
| | 630 | | 602 | 602 |
| –CO ₃ ²⁻ | | | 876 | 871,7 |
| –OH stretching, –OH hydrogen-bonded, NH ₂ as. stretching, N–H stretching in interchain NH–O–C | | 3453 | 3430 | 3419 |
| –CH ₂ - as. | | 2921 | 2924 | 2924 |
| | | 2877 | 2854 | 2852 |
| C=O stretching. ν_{as} (1650-1590) | | 1667 | 1638 | 1634 |
| Deformation δ N–H and ν C–N (AmidII) | | 1599 | 1541 | disappearance |
| Deformation –OH in C–O–H | | 1422 | 1419 | 1423 (intensity increasing) |
| –CH ₂ - deformation δ | | – | 1457 | 1470 |
| C–N stretching coupled with NH in plane deformation (amide III band) | | 1384 | 1384 (intensity decreasing) | disappearance |
| CH ₂ wagging coupled with OH in plane deformation | | 1326 | 1310 | disappearance |
| C–N stretching of the amine (1220-1020) | | 1156 | disappearance | disappearance |
| C–O stretching (–CH–OH, the secondary hydroxyl group) | | 1082 | 1029 | 1030 |
| C–O stretch (–CH ₂ –OH the primary hydroxyl group) | | 1031 | | |
| Deformation N–H in primary amine | | 891 | 895 | disappearance disappearance disappearance |
| | | 941 | disappearance | |
| | | 665 | disappearance | |

The C=O vibration peak of chitosan at 1667 cm⁻¹ shifts to 1638 cm⁻¹ and 1643 cm⁻¹ in a nanocomposite before and after SBF immersion respectively. The peaks at 1031 cm⁻¹ and 1082 cm⁻¹ in chitosan are presented by one peak at 1029 cm⁻¹ in nanocomposite before and 1030 cm⁻¹ after immersion into SBF solution. These changes may be attributed to the formation of hydrogen bonding between OH⁻ groups in HA and –C=O groups in Chitosan. Protonation of chitosan amine functionalities is suggested by the presence of two peaks, both attributed to NH³⁺ groups, namely the antisymmetric deformation at 1638 cm⁻¹ and the symmetric deformation at 1541 cm⁻¹. The initial Amide-I and Amide-II bands were overlapped by these vibrations [30]. Occurrence of the new peak in the nanocomposite spectrum, corresponded to –CH vibration at

1457 cm⁻¹ and its shift to 1470 cm⁻¹ after immersion into SBF solution for 6 days, indicates some interactions between the CS and HA and between ions of the SBF and the nanocomposite. It is noteworthy that all peaks associated with N-H and C-N vibrations in CS have also undergone changes in nanocomposite, indicating interaction between functionalities of CS and HA. Moreover, some of those peaks were disappeared after 6 days in SBF solution (Table 4). The data showed that consisting in nanocomposite Chitosan continues to react with ions of SBF solution via amino groups.

The FTIR spectra of the second group of samples-sodium alginate, HA/CS nanocomposite with 1 w/w% of sodium alginate before and after immersion in SBF are presented in Fig. 5. The main characteristic wave numbers of these nanocomposites are presented in

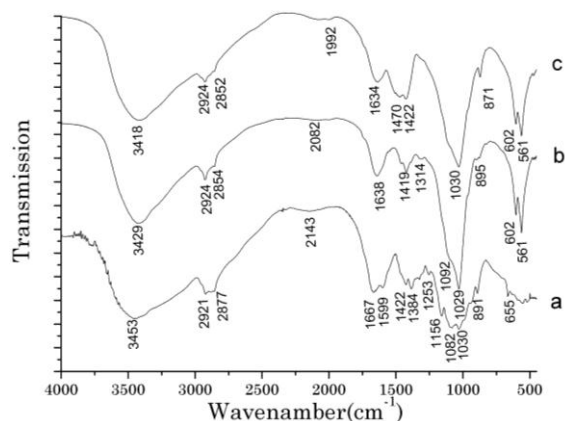


Fig. 4 – FTIR spectra of a) Chitosan, b)HA/CS nanocomposite, c)HA/CS nanocomposite after 6 days in SBF

Table 4. The FTIR spectra of HA/CS /Alg_{1.0} shows no differences compared to HA/CS /Alg_{1.5}, so for the last one spectrum is not given.

The peaks of sodium alginate at 3435 cm⁻¹ and 2923 cm⁻¹ are attributed to stretching vibrations of the free and hydrogen bonded OH⁻ groups in carbon acids respectively [31]. Saturated peak at 1615 cm⁻¹ is assigned to stretching of carbonyl –C=O. IR spectra of major classes of organic compounds [32] in pure sodium alginate and moves back to 1622 cm⁻¹ in the nanocomposite HA/CS/Alg_{1.0} and to 1634 cm⁻¹ after immersion 6 days in SBF solution. Also C–O symmetric stretching in COO⁻ at 1417 cm⁻¹ for alginate reduced to 1420 cm⁻¹ in HA/CS/Alg_{1.0} and to 1425 cm⁻¹ after SBF solution. These changes may be attributed to the formation of bonding

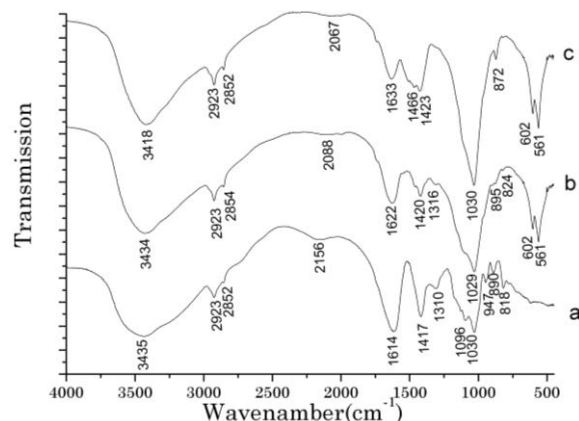


Fig. 5 - FTIR spectra of a) sodium alginate, b) HA/CS /Alg_{1.0} hydrogel, c) HA/CS /Alg_{1.0} hydrogel after 6 days in SBF

between carboxylate anion COO⁻ of alginate and protonated NH₂³⁺ group of CS during the composite formation.

In SBF solution the complexation takes place between these functionalities and ions of SBF. This assumption is confirmed by the changes in the spectrum of HA/CS composite after addition alginate: peaks in 1638 cm⁻¹ and 1541 cm⁻¹, indicating the presence of protonated amino groups in HA/CS, shifted to 1622 cm⁻¹ and 1543 cm⁻¹ in the spectrum HA/CS/Alg_{1.0} and after SBF a last peak disappears. Changes in vibrations of OH in carboxyl groups of alginate at 1340, 1030, 1097, 947, 890 cm⁻¹ also have occurred (Table 3). It can be assumed that carboxyl groups of alginate are ionized to COO⁻ and form H-bond or another bonding during HA/CS /Alg_{1.0} composite formation with the subsequent formation of new bonds while it is in SBF solution.

Table 4 - Characteristic wave number of sodium alginate, HA/CS/Alg_{1.0} and HA/CS/Alg_{1.0} after finding 6 days in SBF solution

| Functional groups | Type of compounds and corresponding vibration peaks (wave numbers) | | |
|---|--|----------------------------|--------------------------------------|
| | Sodium Alginate (Alg) | HA/CS/Alg _{1.0} | HA/CS/Alg _{1.0} (after SBF) |
| –OH stretching in –COOH (3550-3500) | 3435 | 3434 | 3418 |
| –OH stretching in –COOH (hydrogen-bonded, 3300-2500) | 2923 | 2923 | 2924 |
| –CH ₂ –stretching (2870-2845) | 2852 | 2852(intensity increasing) | 2852(intensity increasing) |
| –C=O stretching (Amid1-1650-1590) | 1615 | 1622 | 1634 |
| C–O stretching symm. in COO ⁻ (≈1400-1300) | 1417 | 1420 | 1425 |
| Deformation –OH in COOH (1450-1250) | 1340 | 1304 | disappearance |
| Deformation –O–H in C–O–H (the secondary hydroxyl group, 1125-1030) | 1030 | 1029 | 1031 |
| | 1097 | 1092 | disappearance |
| Deformation of any OH group in COOH (955-890) | 947 | disappearance | disappearance |
| | 890 | 893 (intensity decreasing) | disappearance |

3.4 Structural Integrity Test

Structural integrity is preventing washout of injectable bone cements supporting the original shape and dimensions of implants [33, 34]. The structural integrity of the HA/CS hydrogel, HA/CS/Alg_{1.0} and HA/CS/Alg_{1.5} systems were tested by injection them

into a SBF solution for 1 hour (Fig. 6a), 1, 3 and 7 days (Fig. 6b, c, d). The Petry dishes with SBF solution and hydrogel specimens in the form of rings were continuously shaken (rpm = 60, t = 37 °C) during 7 days.

The decay of the HA/CS hydrogel increased with prolongation of the immersion time. It had completely

lost its form support after 3 day of shaking (Fig. 6c). The HA/CS/Alg_{1.0} specimen remained practically stable saved their initial shape and no obvious decay was observed after 7 days of shaking (Fig. 6d). The HA/CS/Alg_{1.5} specimen began to crumble in 5 days of shaking and lost its initial shape after 7 days (Fig. 6d). This fact obviously is due to the increase in the degree of swelling of the sample with higher content of sodium alginate. Swelling of the composites increases with the increasing alginate content that is confirmed by the

results of our experiment. When the alginate is introduced into HA/CS hydrogel the polyelectrolyte reaction between sodium alginate and HA/CS hydrogel takes place, as proved by FTIR, and enhancing of viscosity is observed. The ability of HA/CS hydrogel to maintain its structural integrity is enhanced with alginate addition, but alginate content more than 1 w/w % leads to reduce of hydrogel plasticity, enhances the swelling and accelerates the shape decay.

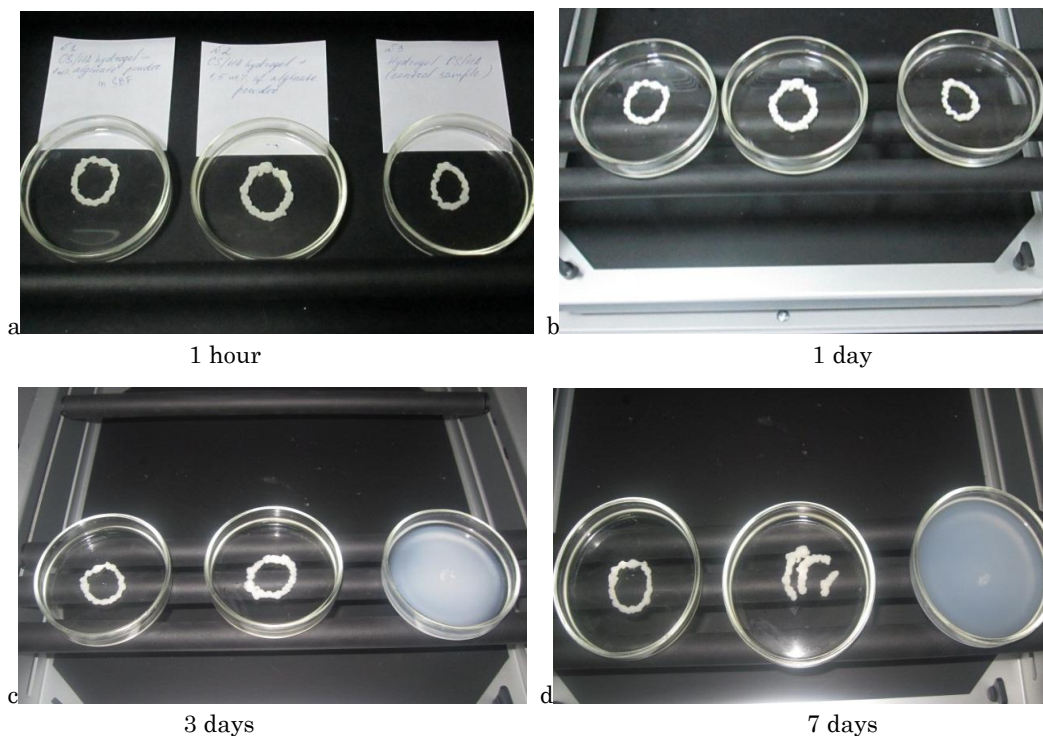


Fig. 6 - Structural integrity test of HA/CS (right), HA/CS/SA_{1.5} (middle) and HA/CS-SA_{1.0} (left) hydrogels

3.5 Swelling and Degradation Study

The swelling and degradation process is an important factor of any biomaterial intended for implantation. For analysis the HA/CS, HA/CS/Alg_{1.0} and HA/CS/Alg_{1.5} samples were partially dried at 37 °C from initial humidity to about 74 w/w % and presented in cubic form. Behavior of the samples was examined in SBF solution in 2 steps: within a short time interval – 5 min, weighting through the 1 minute (Fig. 7 right top) and a long time (5 days, weighting interval was 1 day). The results of the study are shown on Fig. 7. It should be noted that within 5 minutes the swelling degree of all samples was about 3 %. For HA/CS composite it was little changed within 1 day and amounted to 7.6 % during 2 days before the time of degradation beginning. The maximum swelling 18 % for HA/CS/Alg_{1.5} was observed on the first day and 16 % for HA/CS/Alg_{1.0} on the second day of investigations.

It was evident that the degradation of HA/CS occurred due to uniform loss of both organic and inorganic phases. In the case of HA/CS/Alg inorganic component was partially washing out from cross-linked organic matrix, which during the period of the study remained not decayed. In 2 days of experiment all sam-

ples shown weight degradation due to mechanical impact (shaking). In 5 days the degradation rate for HA/CS, HA/CS/Alg_{1.0} and HA/CS/Alg_{1.5} was 8 %, 5.4 % and 7 % respectively. The greatest degree of degradation (8 %) was for HA/CS composite. The degradation decrease for composite material HA/CS/Alg_{1.0} (5.4 %) compared with HA/CS can be explain by forming a matrix of chemically related molecules of Chitosan and

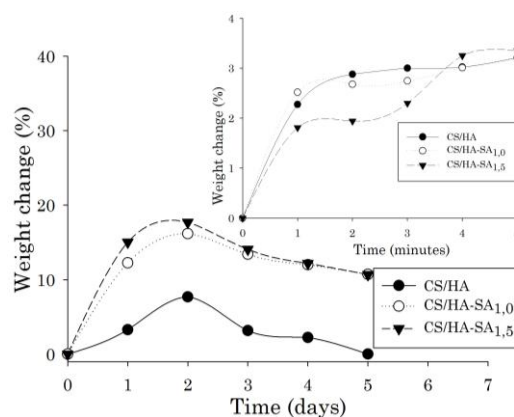


Fig. 7 – Swelling and degradation behavior of HA/CS, HA/CS/Alg_{1.0} and HA/CS/Alg_{1.5} samples

Alginate and cross-linking of polymeric macromolecules with ions of SBF solution. In the case of HA/CS/Alg_{1.5} enhancing of degradation rate up to 7 % compared with HA /CS/Alg_{1.0} was due to the higher degree of swelling.

4. CONCLUSIONS

Hydrogels based on HA and Chitosan with addition of sodium Alginate were synthesized by *in situ* precipitation method. Structure, morphology, chemical and phase composition of the HA/CS/Alg hydrogels were characterized by TEM, FTIR and XRD. HA/CS/Alg hydrogels consist of low crystallinity calcium deficient hydroxyapatite (JCPDS 9-432). The needle-like crystallites had average size 25 nm. When the alginate powder was introduced into HA/CS hydrogel solution the viscosity enhancing of the hydrogel due to polyelectrolyte reaction between Alginate and Chitosan was observed. HA/CS hydrogel forms homogeneous composite with HA powder. Two natural polymers and Ca²⁺ ions partially released from hydroxyapatite formed a matrix by crosslinking the polymer macromolecules through hydroxyl, amino and carbonyl groups. From FTIR in-

vestigations can be assumed that the interaction between functionalities of CS and HA takes place. Carboxyl groups of Alginate are ionized to COO⁻ and form hydrogen or another bonding during HA/CS/Alg composite formation. These processes promote the formation of a more stable structure of hydrogel compared to that of HA/CS.

The structural integrity and degradation tests have demonstrated that the HA/CS hydrogel had completely lost its initial form after 1 day immersion in SBF. After 7 days HA/CS/Alg_{1.0} remained stable in its initial shape and no obvious decay was observed, meanwhile for HA/CS/Alg_{1.5} structural decay was obviously observed. The structural integrity test shows that ability of HA/CS hydrogel to maintain its shape is enhanced with alginate addition, but alginate content more than 1 w/w % reduces the hydrogel plasticity, increases the swelling and accelerates the shape decay.

ACKNOWLEDGMENT

Authors thank gratefully to Prof. Prytula Igor for assistance in FTIR measurements.

Ін'єкційні біополімер-гідроксиапатитні гідрогелі та їх характеристика

Л.Б. Суходуб¹, Г.О. Яновська², В.М. Кузнецов², О.О. Мартинюк², Л.Ф. Суходуб²

¹ ДУ «Інститут мікробіології та імунології імені І.І. Мечникова АМН України», вул. Пушкінська, 14/16, 61057 Харків, Україна

² Сумський державний університет, вул. Римського-Корсакова, 2, 40007 Суми, Україна

Гідрогелі на основі гідроксиапатиту (НА) і хітозану (СS) з додаванням альгінату натрію (Аlg) були синтезовані методом «мокрої хімії». Структура, морфологія, хімічний та фазовий склад гідрогелів НА/СS та НА/СS/Аlg охарактеризовані ТЕМ, FTIR та XRD методами. Гідрогелі мають у своєму складі низько-кристалічний НА (JCPDS 9-432) з середнім розміром голчатих кристалітів 25 нм. Після введення порошку альгінату до складу НА/СS гідрогелю спостерігається підвищення в'язкості композиту в результаті поліелектролітної реакції між альгінатом і хітозаном. Два природних полімери та іони Са²⁺, які частково вивільняються зі складу НА, утворюють полімерну матрицю шляхом зшивання макромолекул полімеру через гідроксильні, карбонільні та аміногрупи. Ці процеси сприяють формуванню більш стабільної структури гідрогелю НА/СS/Аlg порівняно з НА/СS. Дослідження структурної цілісності та деградації матеріалів показали, що НА/СS/Аlg_{1.0} зберігає свою початкову форму протягом 7 днів коливального навантаження в розчині SBF в шейкері (50 об/хв), в той час як НА/СS/Аlg_{1.5} розпадається на фрагменти. НА/СS гідрогель повністю втрачає свою форму через 3 дня експозиції. Таким чином, здатність НА/СS гідрогелю підтримувати форму дефекту при імплантації в кісткову тканину підвищується при додаванні альгінату, але вміст останнього більший, ніж 1 мас. % зменшує пластичність матеріалу, збільшує набухання і прискорює деградацію.

Ключові слова: Гідроксиапатит, Хітозан, Альгінат натрію, Гідрогелі.

Инъекционные биополимер-гидроксиапатитные гидрогели и их характеристика

Л.Б. Суходуб¹, А.А. Яновская², В.М. Кузнецов², А.А. Мартынюк², Л.Ф. Суходуб²

¹ ГУ «Институт микробиологии и иммунологии имени И.И. Мечникова АМН Украины», ул. Пушкинская, 14/16, 61057 Харьков, Украина

² Сумской государственной университет, ул. Римского-Корсакова, 2, 40007 Сумы, Украина

Гидрогели на основе гидроксиапатита (НА) и хитозана (СS) с добавлением альгината натрия (Аlg) были синтезированы методом «мокрой химии». Структура, морфология, химический и фазовый состав НА/СS и НА/СS/Аlg гидрогелей охарактеризованы ТЕМ, FTIR и XRD методами. Гидрогели включают низко-кристаллический НА (JCPDS 9-432) со средним размером игольчатых кристаллитов 25 нм. После введения порошка Аlg в состав НА/СS гидрогеля наблюдается повышение вязкости композита в результате полиэлектролитной реакции между альгинатом и хитозаном. Два природных полимера и

частично высвобождающиеся из состава HA ионы Ca^{2+} формируют полимерную матрицу путем сшивки макромолекул полимеров через гидроксильные, карбонильные аминогруппы. Эти процессы способствуют формированию более стабильной структуры HA/CS/Alg гидрогеля по сравнению с HA/CS. Исследования структурной целостности и деградации материалов показали, что HA/CS/Alg_{1.0} сохраняет свою первоначальную форму после 7 дней колебательной нагрузки в растворе SBF в шейкере (50 rpm), в то время как HA/CS/Alg_{1.5} распадается на фрагменты. HA/CS гидрогель полностью теряет свою форму через 3 дня колебательного воздействия. Таким образом, способность HA/CS гидрогеля поддерживать форму дефекта при имплантации в костную ткань усиливается с добавлением альгината, но содержание последнего более чем 1 мас. % снижает пластичность материала, увеличивает набухание и ускоряет деградацию.

Ключевые слова: Гидроксиапатит, Хитозан, Альгинат натрия, Гидрогели.

REFERENCES

- X. Xu, S. Lü, C. Gao, X. Wang, X. Bai, N. Gao, M. Liu, *Chem. Eng. J.* **240**, 331 (2014).
- N. Hunt, L. Grover, *Biotechnol. Lett.* **32**, 733 (2010).
- B. Balakrishnan, A. Jayakrishnan, *Biomaterials* **26**, 3941 (2005).
- J.L. Drury, D.J. Mooney, *Biomaterials* **24**, 4337 (2003).
- F.S. Palumbo, G. Pitarresi, C. Fiorica, S. Rigogliuso, G. Ghersi, G. Giammona, *Mater. Sci. Eng.: C* **33** No 5, 2541 (2013).
- Y. Qiu, K. Park, *Adv. Drug Delivery Rev.* **64**, 49 (2012).
- R. Fei, J.T. George, J. Park, A.K. Means, M.A. Grunlan, *Soft Matter* **9**, 2912 (2013).
- X. Xu, S. Lü, C. Gao, X. Wang, X. Bai, N. Gao, M. Liu, *Chem. Eng. J.* **240**, 331 (2014).
- M. Jaiswal, S. Lale, N. G. Ramesh, V. Koul, *React. Funct. Polym.* **73**, 1493 (2013).
- S. Sharifi, S.B.G. Blanquer, T.G. van Kooten, D.W. Grijpma, *Acta Biomater.* **8**, 4233 (2012).
- S. Mollazadeh, J. Javadpour, A. Khavandi, *Ceram. Int.* **33**, 1579 (2007).
- W.S. Wan Ngah, *Chem. Eng. J.* **143**, 62 (2008).
- Y. Murata, Y. Kodama, T. Isobe, K. Kofuji, S. Kawashima, *Int. J. Polym. Sci.* **2009**, ID 729057 (2009).
- I.M. El-Sherbiny, *Carbohydr. Polym.* **80**, 1125 (2010).
- I.M. El-Sherbiny, E.M. Abdel-Bary, *J. Appl. Polym. Sci.* **115**, 2828 (2010).
- Y. Han, Q. Zeng, H. Li, J. Chang, *Acta Biomater.* **9**, 9107 (2013).
- R.A.A. Muzzarelli, *Carbohydr. Polym.* **83**, 1433 (2011).
- Y. Han, Q. Zeng, H. Li, J. Chang, *Acta Biomater.* **9**, 9107 (2013).
- T. Kokubo, H. Kushitani, S. Sakka, T. Kitsugi, T. Yamamuro, *J. Biomed. Mater. Res.* **24**, 721 (1990).
- H. P. Klug, L. E. Alexander, *X-Ray Diffraction Procedures: For Polycrystalline and Amorphous Materials* (New York: Wiley, 1974).
- S.N. Danilchenko, O.G. Kukhareno, C. Moseke, *Cryst. Res. Technol.* **37**, 1234 (2002).
- S.N. Danilchenko, O.V. Kalinkevich, V.N. Kuznetsov, *Cryst. Res. Technol.* **45**, 685 (2010).
- F.H. Chung, *J. Appl. Crystallogr.* **8** No 1, 17 (1975).
- I. Manjubala, S. Sheler, J. Bossert, *Acta Biomater.* **2**, 75 (2006).
- I. Rehman, W. Bonfield, *J. Mater. Sci.: Mater. Med.* **8** No 1, 1 (1997).
- S. Nayar, A. Sinha, *Colloid Surf. B* **35** No 1, 29 (2004).
- V.K. Malesu, D. Sahoo, P.L. Nayak, *Int. J. Appl. Ceram. Tech.* **2** No 3, 402 (2011).
- Li Baoqiang, W. Yongliang, J. Dechang Jia, Yu Zhou, *J. Biomat. Sci. Polym. Ed.* **22**, 505 (2011).
- I.F. Amaral, P.L. Granja, M.A. Barbosa, *J. Biomat. Sci. Polym. Ed.* **16**, 1575 (2005).
- P.L. Granja, L. Pouysegue, D. Deffieux, G. Daude, B. De Jeso, C. Labrugere, C. Baquey, M.A. Barbosa, *J. Appl. Polym. Sci.* **82**, 3354 (2001).
- C. Kalasanathan, N. Selvacumar, V. Naidu, *Ceram. Int.* **38**, 571 (2012).
- B.N. Tarasevych, *IK spektry osnovnykh klassov organicheskikh soedinenij* (Moskva: 2012).
- Q. Lin, X. Lan, Y. Li et al., *J. Mater. Sci-Mater. M* **21**, 3065 (2010).
- Y.J. Diani, F.K. Tzong, D.W. Hong, J.C. Yang, S.Y. Lee, *Carbohydr. Polym.* **89**, 1123 (2012).